Hindawi
Advances in Meteorology
Volume 2018, Article ID 9081910, 10 pages
https://doi.org/10.1155/2018/9081910

Research Article

Numerical Study of a Southwest Vortex Rainstorm Process Influenced by the Eastward Movement of Tibetan Plateau Vortex

Xiaoli Liu,[1] **Endian Ma**,[1] **Zhibin Cao**,[2] **and Shuanglong Jin**[3]

[1]*Key Laboratory of Meteorological Disaster of Ministry of Education, Key Laboratory for Aerosol-Cloud-Precipitation of China Meteorological Administration, and Collaborative Innovation Center on Forecast and Evaluation of Meteorological Disasters, Nanjing University of Information Science and Technology, Nanjing 210044, China*
[2]*Purple Mountain Observatory, Nanjing 210008, China*
[3]*State Key Laboratory of Operation and Control of Renewable Energy & Storage Systems, China Electric Power Research Institute, Beijing 100192, China*

Correspondence should be addressed to Shuanglong Jin; shuanglongjin@126.com

Received 4 November 2017; Revised 27 March 2018; Accepted 2 April 2018; Published 3 May 2018

Academic Editor: Bin Yong

Copyright © 2018 Xiaoli Liu et al. This is an open access article distributed under the Creative Commons Attribution License, which permits unrestricted use, distribution, and reproduction in any medium, provided the original work is properly cited.

A number of studies revealed the possible eastward movement of the Tibetan Plateau low-pressure system in summer and indicated the enhancement effect of this process on the southwest vortex in the Sichuan Basin, which can induce strong convective precipitation and flood events in China. In this study, a numerical simulation of a southwest vortex rainstorm process was performed. The results show that the low-pressure system originated from the Tibetan Plateau affects the southwest vortex mainly at the middle level, causing the strength increase of southwest vortex (SWV), and acts as a connection between the positive vorticity centers at the upper and lower layers. For the microscopic cloud structure, the vertical updraft of the cloud cluster embedded in the SWV increases as the low-pressure system from the plateau arrives at the Sichuan Basin. Vapor and liquid cloud water at the lower level are transported upward, based on which the ice cloud at the upper level and the warm cloud at the lower level are joined to create favorable conditions for the growth of ice crystals. As the ice crystals grow up, snow and graupel particles form, which substantially elevates the precipitation. This effect leads to the rapid development of SWV rainstorm clouds and the occurrence of precipitation. In addition to the effect of the plateau vortex, the subsequent merging of the convective clouds is another important factor for heavy rainfall because it also leads to development of convective clouds, causing heavy rainfall.

1. Introduction

The southwest vortex (SWV) is one of the major weather systems that affect precipitation in China; early studies date back to the 1940s. The SWV can be triggered or intensified by the low-pressure system moving out of the plateau, with suitable weather conditions in the Sichuan Basin [1]. It is found that the eastward-moving plateau vortex and the SWV coupling vertically promote the development of the SWV [2]. This vertical interconnection forces the intensification of the updraft velocity in cloud, leading to the growth of SWV [3]. When combined with favorable atmospheric vapor conditions, the SWV easily triggers a series of mesoscale convective activities, affecting the large-area rainfall process of eastern China, causing floods and severe economic losses [1, 4–21].

The influence of the eastward movement of the low-pressure plateau system on the convective clouds embedded in the SWV and the accompanied release of latent heat associated with cloud physics is important for the development and eastward shift of the SWV [22–25], which is particularly true for the development of positive vorticity in low-mid layers during the occurrence of heavy precipitation [26–28]. Although topographical dynamics only form a shallow SWV, cloud physics and the accompanied latent heat release induce adequate development of the SWV [4, 29].

Based on existing research results, the eastward movement of the low-pressure plateau system might couple with the SWV and lead to the occurrence of heavy rainfall. During this process, microphysical processes influence the development and evolution of the dynamic and thermodynamic structures

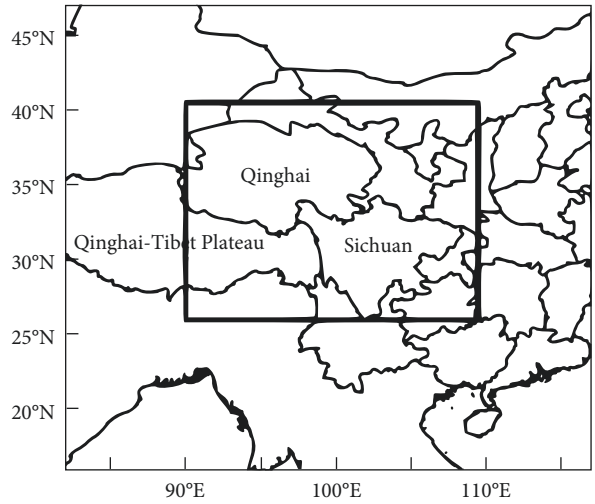

Figure 1: Case simulation domains; the outer frame is the D01 area and the inner frame is the D02 area.

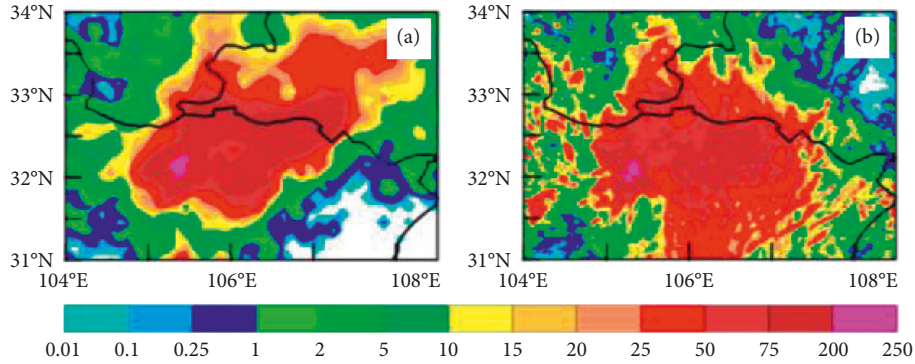

Figure 2: Twenty-four-hour accumulative precipitation from 06:00 UTC on June 27 to 06:00 UTC on June 28, 2015: (a) observation data; (b) simulation result (unit: mm).

of the convective system and micro- to mesoscale weather systems. Therefore, the study of the interaction between the eastward-moving low-pressure plateau system and the SWV especially the macro- and microevolution of convective clouds during this process is of great significance to understand the physical mechanism behind heavy rainfall due to the SWV.

2. Case and Model Description

From June 27 to 28, 2015, part areas in the northeastern Sichuan Province suffered large-scale heavy rainfall with thunder and lightning, with a short-term strong gust in some areas. Certain towns and counties received precipitation more than 100 mm, reaching a maximum of 247 mm. This intense rainfall severely impacted northeastern Sichuan; numerous towns and counties were flooded, many roads were destroyed, and nearly 20000 people were evacuated. Landslides and other disasters due to the heavy rain also threatened the safety of residents, causing huge economic losses.

In this study, the WRFV3.4 model was used to perform numerical simulations. The start and end times of the case simulation were 06:00 UTC on June 27 to 06:00 UTC on June 28, 2015. A double-layer, two-way-nested scheme centered at 33.4°N and 99.7°E was adopted (Figure 1). The first layer (D01) included 450×390 lateral grid points with 9 km spacing, and the second layer (D02) contained 646×550 points with 3 km spacing. The topographical information used was the 2 m, 30 s global data from the United States Geological Survey (USGS). Boundary conditions were imposed on the fine mesh by the coarse mesh. The following parameterizations were used: RRTM (rapid radiative transfer model) longwave radiation [30], Dudhia shortwave radiation [31], the revised MM5 (Mesoscale Model 5) Monin–Obukhov surface layer scheme [32], the Noah land surface model [33], and the YSU (Yonsei University scheme) planetary boundary layer [34], and the Grell–Devenyi ensemble cumulus scheme [35] was employed only for D01. The Milbrandt–Yau double-moment 7-class scheme [36, 37] was chosen for microphysics parameterization.

Figure 2 shows the 24-hour cumulative precipitation from 06:00 UTC on June 27 to 06:00 UTC on June 28, 2015, with Figure 2(a) being the observation record and Figure 2(b) being the simulation result. The comparison shows that the simulated precipitation area largely coincides with the observation, particularly in regions of heavy rainfall. The simulated rainfall amount and the location of the maximum precipitation correspond with the observation: the observed precipitation center is at 32.01°N and 105.46°E, whereas the

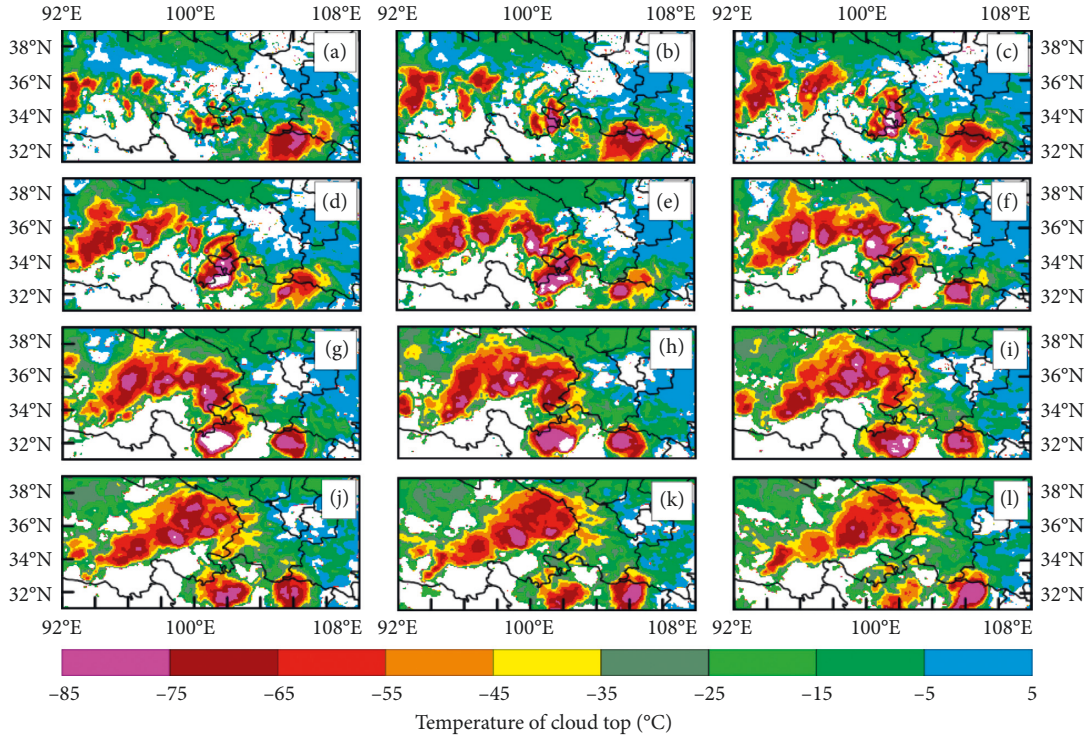

Figure 3: FY-2F cloud top temperatures on June 27, 2015 (unit: ˚C): (a) 07:00 UTC; (b) 08:00 UTC; (c) 09:00 UTC; (d) 10:00 UTC; (e) 11:00 UTC; (f) 12:00 UTC; (g) 13:00 UTC; (h) 14:00 UTC; (i) 15:00 UTC; (j) 16:00 UTC; (k) 17:00 UTC; (l) 18:00 UTC.

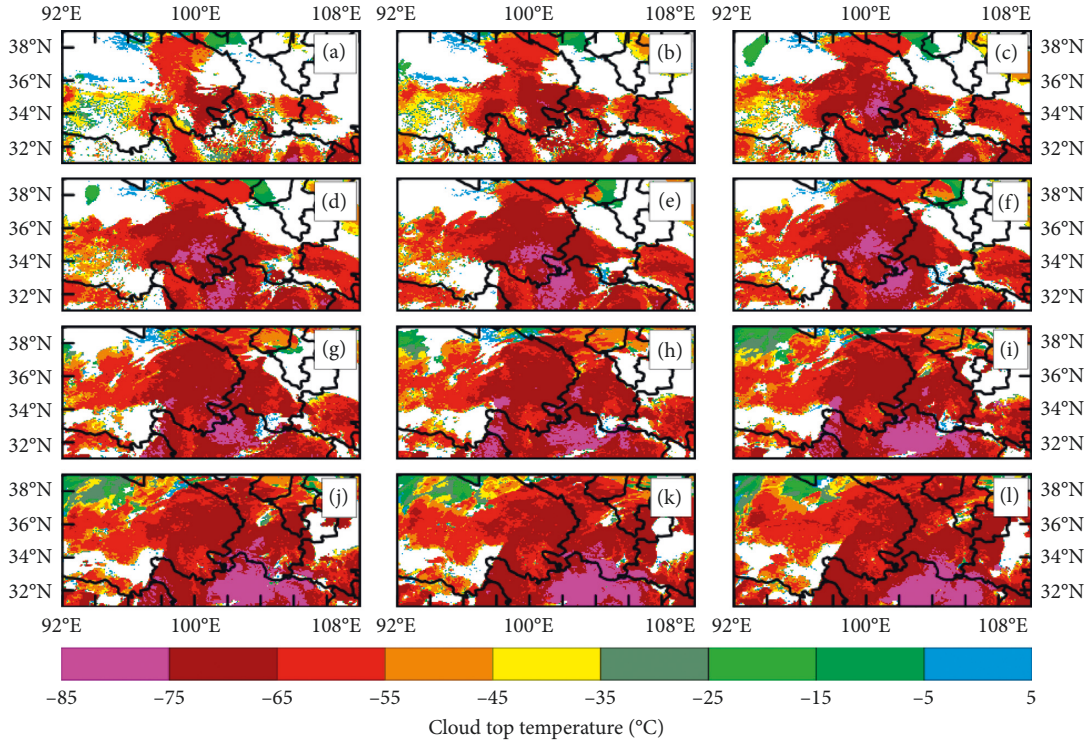

Figure 4: Simulated cloud top temperatures on June 27, 2015 (unit: ˚C): (a) 07:00 UTC; (b) 08:00 UTC; (c) 09:00 UTC; (d) 10:00 UTC; (e) 11:00 UTC; (f) 12:00 UTC; (g) 13:00 UTC; (h) 14:00 UTC; (i) 15:00 UTC; (j) 16:00 UTC; (k) 17:00 UTC; (l) 18:00 UTC.

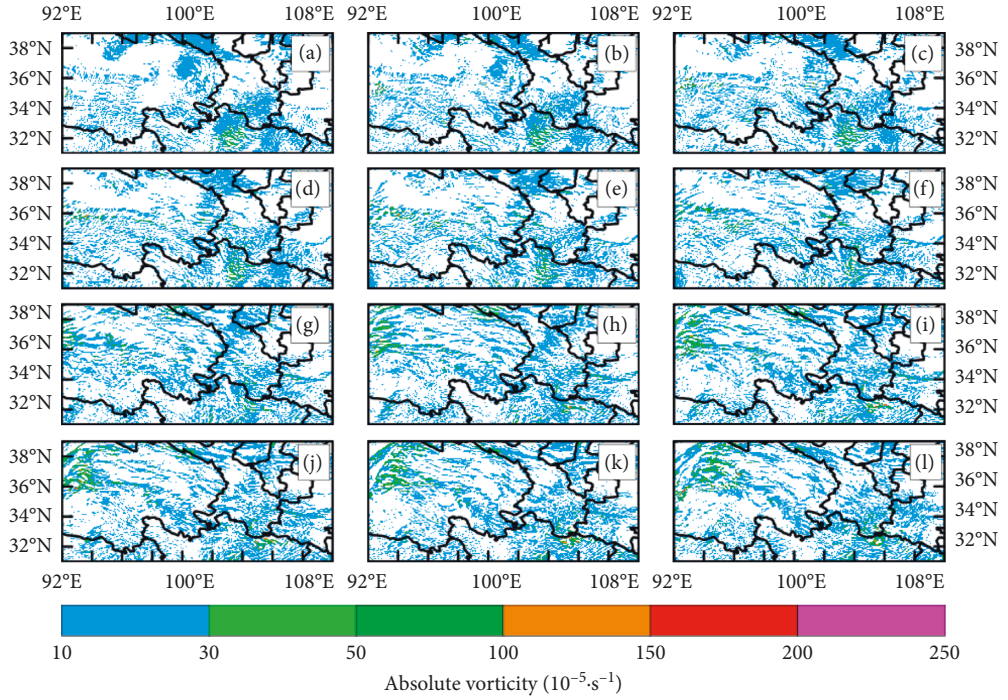

Figure 5: Distribution of absolute vorticity at 8 km on June 27: (a) 07:00; (b) 08:00; (c) 09:00; (d) 10:00; (e) 11:00; (f) 12:00; (g) 14:00; (h) 16:00; (i) 17:00; (j) 18:00; (k) 19:10; (l) 20:00.

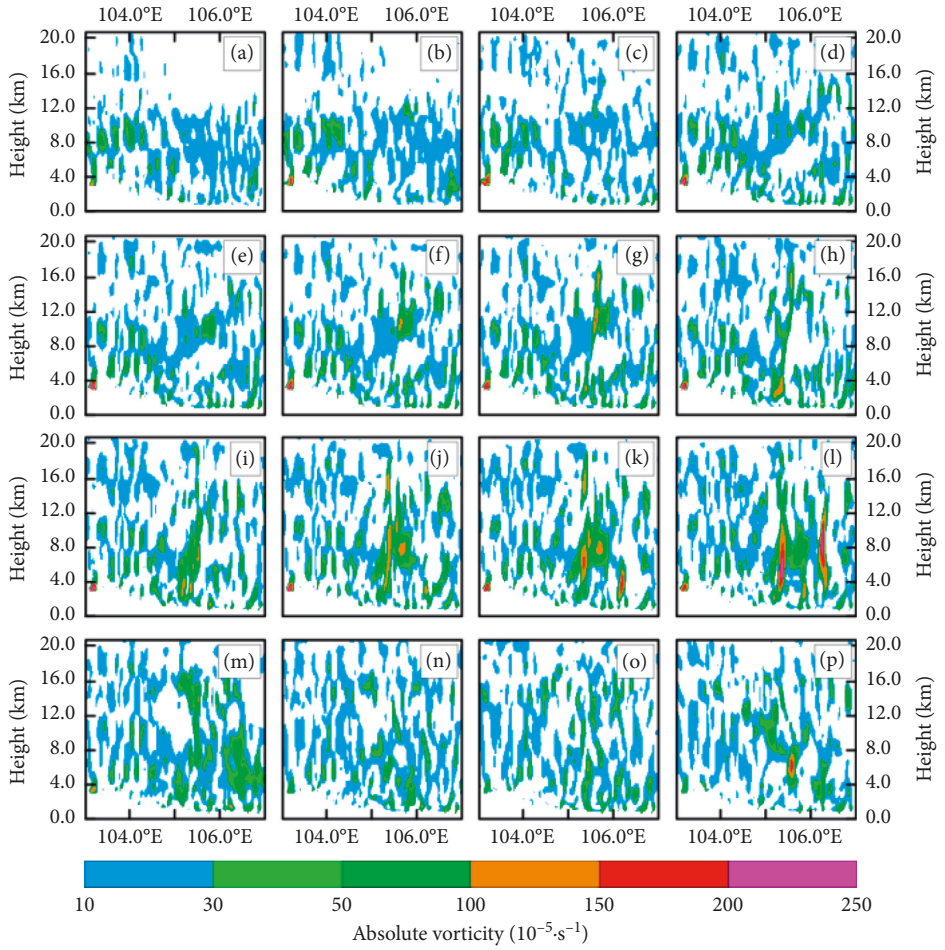

Figure 6: Vertical distribution of absolute vorticity at 32.1°N on June 27: (a) 07:00; (b) 09:00; (c) 11:00; (d) 13:00; (e) 13:10; (f) 13:20; (g) 13:30; (h) 14:00; (i) 14:30; (j) 15:00; (k) 15:10; (l) 15:30; (m) 16:30; (n) 17:30; (o) 19:10; (p) 21:30.

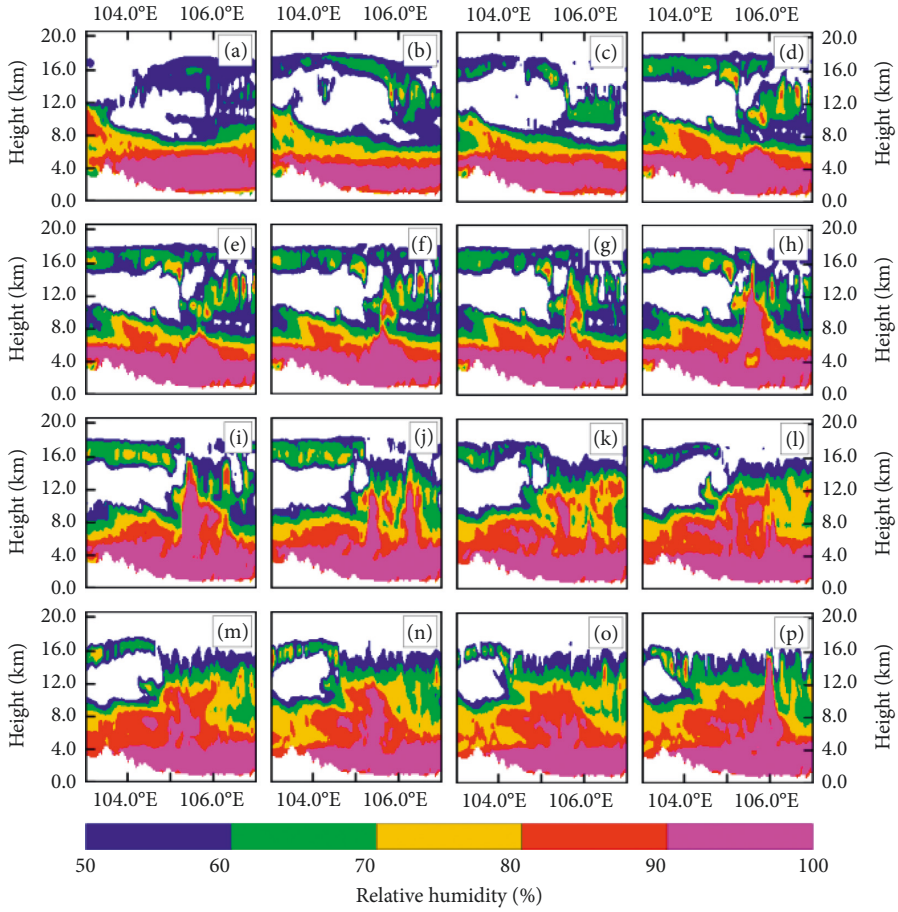

Figure 7: Vertical distribution of relative humidity at 32.1°N on June 27: (a) 07:00; (b) 09:00; (c) 11:00; (d) 13:00; (e) 13:10; (f) 13:20; (g) 13:30; (h) 14:00; (i) 15:00; (j) 16:00; (k) 17:00; (l) 18:00; (m) 19:00; (n) 20:00; (o) 21:00; (p) 22:00.

simulated center is at 32.15°N and 105.31°E. Basically, the simulated rainfall at ground agrees well with the reality in the northeastern Sichuan Basin.

Based on the cloud top temperatures evolvement (Figure 3), several convective cloud clusters are present from 07:00 to 12:00 UTC on June 27, from western Qinghai to the Qinghai/Sichuan border. As the convective clouds in western Qinghai continue to move eastward, the clouds at the Qinghai/Sichuan border continue to grow and shift south. At 12:00 UTC, the latter begins to strengthen as the convective clouds in western Sichuan move south to 32°N, that is, arrive at the latitude of the convective clouds of eastern Sichuan. By 14:00 UTC, the convective clouds in western Sichuan move eastward and weaken, while those in the east keep growing. By 17:00 UTC, the convective clouds in western Sichuan disappear and the ones in the east grow significantly, developing into a deep convective system, along with the SWV. This development and strengthening of convective clouds in the SWV is accompanied by the eastward movement of the convective plateau system.

3. Numerical Simulation Results

3.1. Simulated Characteristics of the Eastward Movement of Convective Plateau Clouds. Figure 4 shows the simulated cloud top temperatures from June 27 to 28, 2015. Compared with the satellite-observed cloud top temperature, it can be seen that the simulation reproduces the distribution and evolvement characteristics of the convective clouds in western Qinghai, the southward movement of the clouds in eastern Qinghai, and the strengthening of convective clouds in eastern Sichuan.

3.2. Simulation of the Eastward Movement of the Plateau Vortex. There is a large area of positive vorticity spanning the downhill eastern plateau and northern Sichuan Basin at 07:00 UTC in the vicinity of 103°E (Figure 5). During this period, a strong positive vorticity forms in western Qinghai, which keeps moving east. At 10:00 UTC, this positive vorticity shifts east to ~103°E and meets the local positive vorticity. The latter strengthens and moves to ~104°E. Subsequently, the vorticity center of the Sichuan Basin continues to move eastward accompanied by the eastward movement of the plateau vortex and significant strength enhancement of the positive vorticity in downstream. At 14:00 UTC, an intense positive vorticity center forms at ~106°E, which strengthens with time and grows in range. By 16:00 UTC, the positive vorticity region of the northern Sichuan Basin further extends east, reaching a stronger vorticity

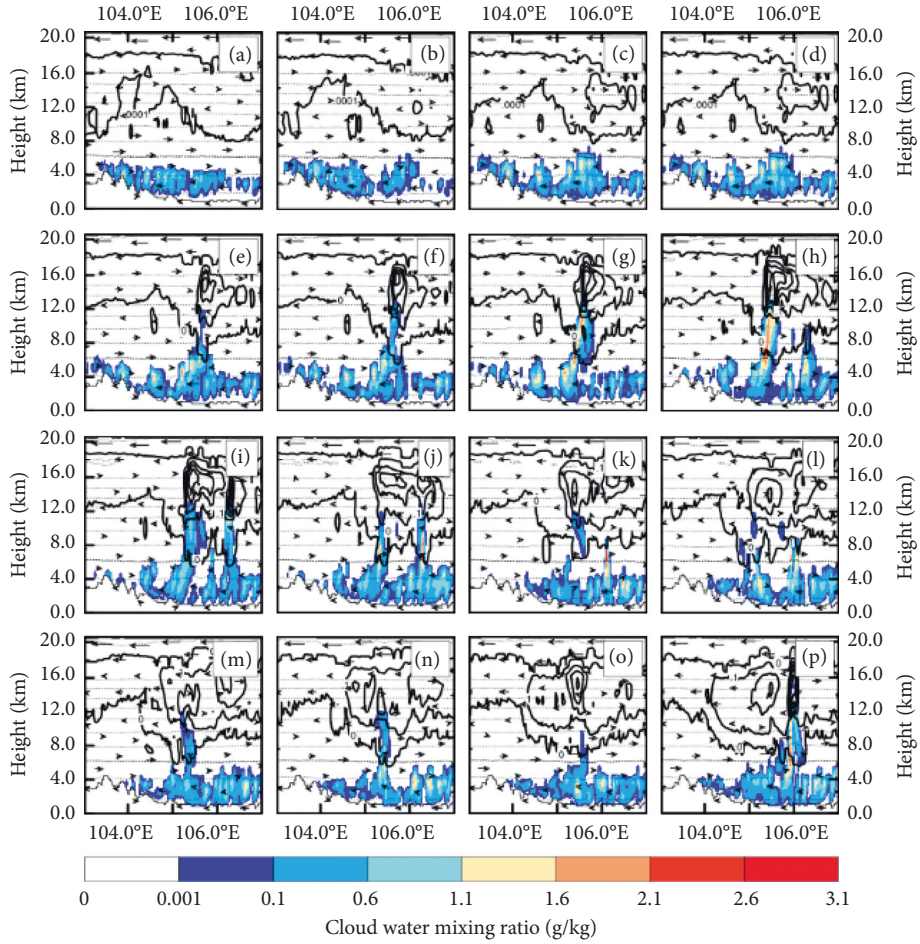

Figure 8: Longitude-height cross section of cloud droplet and ice crystal mixing ratio at 32.1°N; the mixing ratio of cloud droplets is represented by shade color; the mixing ratio of ice crystals is represented by solid lines (start value: 0.0001 g/kg; interval: 0.5 g/kg from 0.1 to 3.1 g/kg); the wind vector is represented by arrows; the thick dotted line is the 0°C isotherm on June 27: (a) 11:00; (b) 12:00; (c) 13:00; (d) 13:10; (e) 13:20; (f) 13:30; (g) 14:00; (h) 15:00; (i) 15:30; (j) 16:00; (k) 17:00; (l) 18:00; (m) 19:00; (n) 20:00; (o) 21:00; (p) 22:00.

center. Thereafter, the plateau vortex still moves east; however, the enhancement of the SWV gradually decreases.

The vertical distribution of vorticity (Figure 6) shows positive vorticity regions in both upper and lower levels above the Sichuan Basin in the early stage, with the upper ones at 10–14 km and the lower ones below 6 km. At 11:00 UTC, there are several positive vorticity centers over the plateau located about 8~10 km, and the positive vorticity center has an eastward-moving tendency. During its eastward shift along the eastern slope of the plateau, the vertical range of the vorticity increases as the altitude decreases; however, there is still no positive center around 8~10 km over the Sichuan area. During 13:00–13:30, under the influence of the eastward plateau vortex, a positive vortex center appeared at 8~10 km over the Sichuan Basin and intensified with time. By 14:00 UTC, the plateau vortex connects the upper and lower positive vorticity centers of the Sichuan Basin. The updraft velocity in the convective clouds increases rapidly, and the vertical extent of the clouds significantly thickens. At 14:30 UTC, the updraft velocity further intensified with the thickness of the positive vorticity area and convective clouds vertically extend. During this period, the positive vorticity above the plateau still moves eastward and meets downstream convective clouds at 15:30 UTC, with the vertical thickness of this originally shallow vorticity center located at ~106°E increasing and the updraft inside strengthening. After 15:30 UTC, the eastward shift of the vortex above the plateau gradually diminishes.

From the vertical distribution of relative humidity (Figure 7), it can be found that, in the early stage, the layers below 6 km are rather humid. A wet layer with 80–90% relative humidity exists at 8–12 km above the plateau, which is related to the positive vorticity over the plateau at this height. At this time, there is a center of 60–70% humidity located at 12–16 km above the Sichuan Basin, which corresponds to the positive vorticity center around this level. From 11:00 to 14:00 UTC, the relative humidity above the plateau shows an observable shift to eastern Sichuan. Influenced by the eastward movement of the plateau vortex, the upper wet layer of western Sichuan gradually deepens, that is, the upper and lower cloud clusters connect and the convection strengthens. At the same time, the high relative humidity at the middle level tends to expand east. A new center of high relative humidity occurs at the east of 106°E

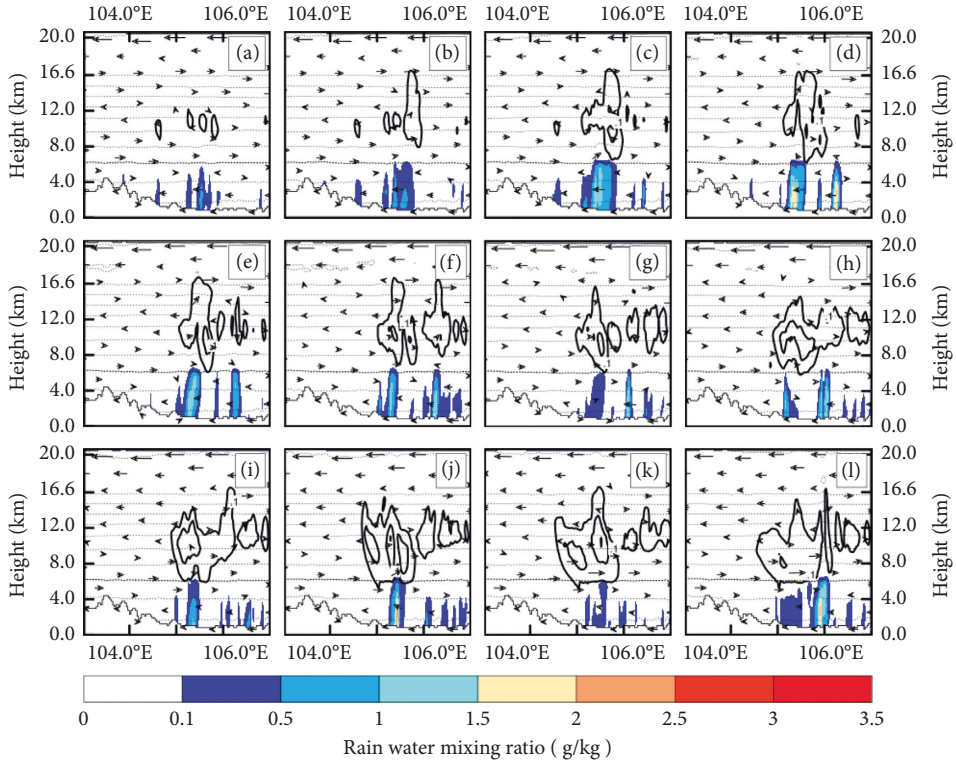

FIGURE 9: Longitude-height cross section of rain and snow mixing ratio at 32.1°N; the mixing ratio of rain is represented by shade color; the mixing ratio of snow is represented by solid lines (start value: 0.0001 g/kg; interval: 0.5 g/kg from 0.1 to 3.1 g/kg); the wind vector is represented by arrows; the thick dotted line is the 0°C isotherm on June 27: (a) 13:00; (b) 13:30; (c) 14:00; (d) 15:00; (e) 15:30; (f) 16:00; (g) 17:00; (h) 18:00; (i) 19:00; (j) 20:00; (k) 21:00; (l) 22:00.

after 15:00 UTC, reaching a height of 12 km. New convective cells also form around this location and develop with time.

Previous analyses showed that the upper and lower positive vorticity centers over eastern Sichuan are not connected between 11:00 and 13:00 UTC. During this period, the updraft is very weak and cloud liquid water is present only below the 0°C isotherm (~6 km), with small amounts of ice at high altitude (Figure 8). The maximum cloud liquid and ice water contents at 13:00 UTC are 1.6 and 0.6 g/kg, respectively. During 13:00–13:30, accompanied by the intensification of vorticity and the increase of relative humidity around 105.5°E, the cloud at this area develops to deeper extent, with the liquid cloud water apparently be transported upward. At 14:00 UTC, the positive vorticity regions in the upper and lower levels, with the increase of vertical thickness of the clouds and the intensification of updraft, transport a large amount of cloud liquid water up, reaching 12 km. This massive upward movement of supercooled cloud liquid water increases the amount of cloud ice. By now, the maximum mixing ratio of liquid and ice water reach 2.0 and 1.5 g/kg, respectively. As the supercooled cloud liquid water transforms into ice at higher altitude, the formation of ice-phase particles enhances. At 15:00 UTC, the center of supercooled cloud liquid water is elevated to ~8 km and the maximum water content reaches 2.1 g/kg. The maximum ice water content also increases to 1.5 g/kg. At this time, the continued eastward motion of the positive vorticity at 8 km strengthens the convective clouds downstream. From 15:00 to 15:30 UTC, the liquid and ice water contents of the former convective clouds significantly decrease, while those of the latter increase. After 15:30, the influence of the upstream positive vortex decreases, and the mixing ratio of cloud droplets and ice crystals decreases gradually.

Figure 9 shows the vertical distribution of the rain and snow water content along 32.1°N. There is little rain and snow in the clouds above the eastern plateau and the Sichuan Basin during the early period. By 13:30 UTC, with the attendance of the plateau vortex, the updraft in the clouds and the rain and snow water contents increase. The intensity of the upward velocity continues to increase thereafter. At 14:00 UTC, the snow distribution drops toward the 0°C isotherm and the center altitude of the snow water content also decreases. At 15:30 UTC, the snow water content of the convective clouds increases with the continued eastward shift of the plateau vortex around 8~10 km and its center altitude moves up.

Graupel particles appear later with respect to other ice-phase particles (13:30 UTC; Figure 10). At 14:00 UTC, the graupel water content increases with the intensity of the updraft and reaches 5 g/kg at 15:00 UTC. By 15:30 UTC, the graupel evolves upward to 16 km with the center moving up to ~10 km. Graupel particles also start to appear in the rear convective clouds at this time, and the mixing ratio reaches 5 g/kg. After 15:30 UTC, the graupel water content of the convective cloud cluster decreases, and there is

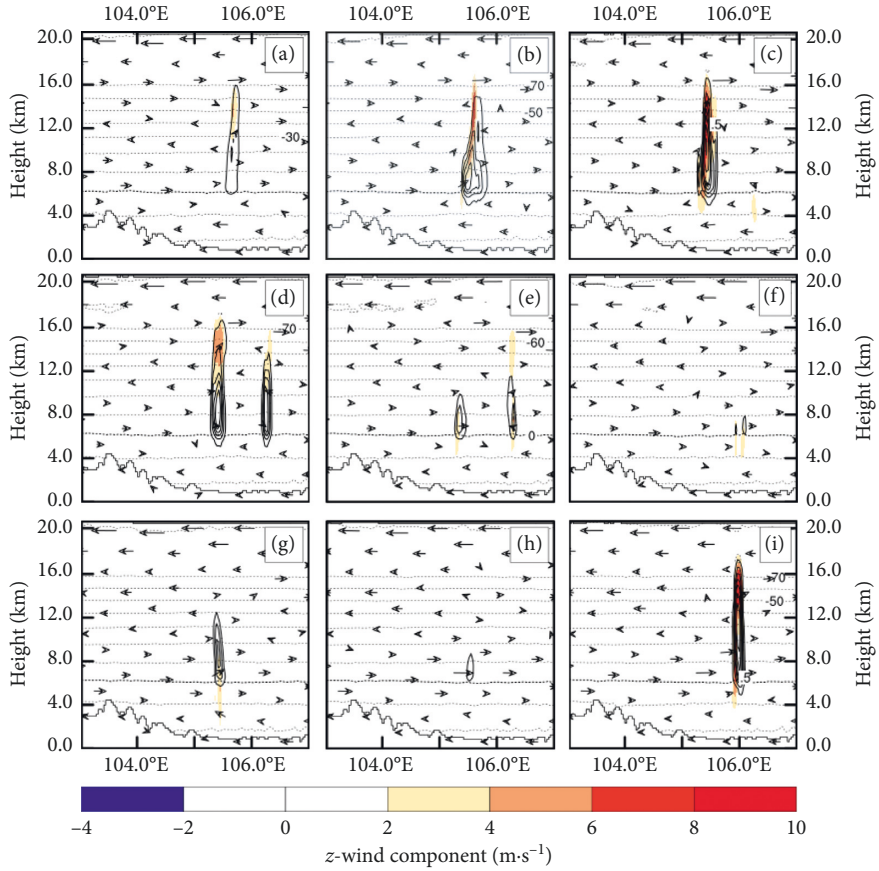

Figure 10: Longitude-height cross section of graupel mixing ratio at 32.1°N; the mixing ratio of graupel is represented by solid lines (start value: 0.5 g/kg; interval: 1 g/kg); the updraft velocity is represented by shaded color; the thick dotted line is the 0°C isotherm on June 27: (a) 13:30; (b) 14:00; (c) 15:00; (d) 15:30; (e) 16:00; (f) 18:00; (g) 19:00; (h) 20:00; (i) 21:00.

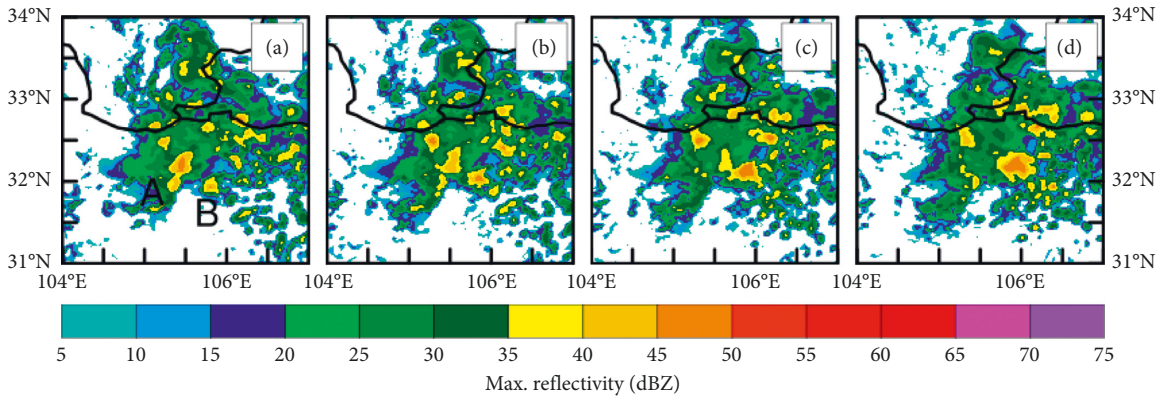

Figure 11: Maximum radar reflectivity for merging of precipitation clouds A and B on June 27: (a, e) 21:00 UTC; (b, f) 21:30 UTC; (c, g) 22:00 UTC; (d, h) 22:30 UTC (unit: dBz).

a significant increase around 21:00, which is the development of the local cloud system.

3.3. Analysis of Convective Cloud Merging. After the effect of the plateau vortex on the rainstorm clouds of the Sichuan Basin weakens, the convective cloud cluster continues to evolve. At 21:00 UTC on June 27, the convective cloud cluster A strengthens over the precipitation center (Figure 11), which enhances the ground precipitation below. This cloud cluster shifts east. A new convective cell B (31.9°N, 105.7°E) emerges to the lower right of A, grows, and moves north. At 21:30 UTC, cluster A begins to merge with B; A weakens and B strengthens. The rainfall above the precipitation center decreases as B moves east. By 22:00 UTC, cloud A generally develop into the dissipate stage and B continues to grow. At 22:30 UTC, the two clusters fully merge; thereafter, the new cluster keeps moving east and merges with the other new clusters, bringing heavy rain to the eastern region. This

intense rainfall over northeastern Sichuan therefore occurs in two stages: the evolution of precipitation clouds accompanied by the eastward migration of plateau convective clouds and the growth of a cloud cluster due to merging of convective clouds over the rainfall region.

4. Conclusions and Discussion

(1) To the area and case we studied, the vortex system of the Qinghai-Tibet Plateau shows eastward movement, which is most prominent for the vortex at the middle level above the plateau. When the plateau vortex moves east to the Sichuan Basin, the vertical thickness of the SWV increases and the positive vorticity centers at the lower and upper levels connect. At the same time, the cloud thickness and strength increase. It is shown that the intensification and deep development of the cloud cluster in the Sichuan Basin are significantly accompanied by the eastward movement of the low-pressure system originated from the Tibet Plateau.

(2) The eastward movement of the plateau vortex and SWV is accompanied by the variations in the macro- and microphysical structures of the clouds. As the upper- and lower-level clouds merge, the supercooled cloud water breaks through the originally dry air layer and moves upward, which activates the growth of ice-phase crystals in the clouds including the transformation of ice crystals to snow and that of snow to graupel, providing the condition to the occurrence of precipitation and the further development of the convective cloud system in the Sichuan Basin.

(3) The positive vorticity center at the middle level extends downstream and affects the development of nascent convective cells in the cloud cluster. The updraft in these new cells increases, which speeds up the formation and growth of precipitation particles in the clouds. When the influence of the plateau vortex wears off, the convective clouds locally maintain their growth for a considerable period of time and merge with new convective clouds, enhancing the updraft velocity and cloud evolution.

Conflicts of Interest

The authors declare that they have no conflicts of interest.

Acknowledgments

This research was supported by the National Natural Science Foundation of China (41375137, 41505118, and 41505121); the Open Funding from the Key Laboratory of Meteorological Disaster of Ministry of Education, China (KLME1205); and the Science Technology Foundation of State Grid Corporation of China (1704-00203).

References

[1] T. Yasunari and T. Miwa, "Convective cloud systems over the Tibetan Plateau and their impact on meso-scale disturbance in the Meiyu/Baiu frontal zone," *Journal of the Meteorological Society of Japan*, vol. 84, no. 4, pp. 783–803, 2006.

[2] Q. Miao, B. Liu, and L. X. Yuan, "Characteristic analysis of the coupling interaction between the weather system over the Tibetan Plateau and the shallow weather system at its lee," *Plateau and Mountain Meteorology Research*, vol. 9, no. 3, pp. 18–22, 1999, in Chinese.

[3] C. H. Zhou, Q. Y. Gu, and G. B. He, "Diagnostic analysis of vorticity in a heavy rain event under interaction of plateau vortex and southwest vortex," *Meteorological Science and Technology*, vol. 37, no. 5, pp. 538–544, 2009, in Chinese.

[4] Z. M. Chen, W. B. Min, Q. Miao, and G. B. He, "A case study on coupling interaction between plateau and southwest vortexes," *Plateau Meteorology*, vol. 23, no. 1, pp. 75–80, 2004, in Chinese.

[5] S. M. Fu, J. H. Sun, S. X. Zhao, W. L. Li, and B. Li, "A study of the impact of the eastward propagation of convective cloud systems over the Tibetan Plateau on the rainfall of the Yangtze-Huai River basin," *Acta Meteorologica Sinica*, vol. 69, no. 4, pp. 581–600, 2011, in Chinese.

[6] B. He, F. He, X. H. Fan, and X. H. Zhang, "Diagnostic analysis on a Meiyu front rainstorm process in mid- and low-reaches of Yangtze River," *Plateau Meteorology*, vol. 32, no. 4, pp. 1071–1083, 2013, in Chinese.

[7] J. X. Jiang and M. Z. Fan, "Convective clouds and mesoscale convective systems over the Tibetan Plateau in summer," *Chinese Journal of Atmospheric Sciences*, vol. 26, no. 2, pp. 263–270, 2002, in Chinese.

[8] Y. H. Jiang, Q. Du, D. J. Zhao, Y. He, and J. Li, "Study on structure characteristic of southwest vortex accompanying with heavy rainstorm in East Sichuan Basin," *Plateau Meteorology*, vol. 31, no. 6, pp. 1562–1573, 2012, in Chinese.

[9] L. Kang, L. P. Hao, and J. L. Niu, "Feature analysis on southwest vortex of triggering rainstorm," *Plateau Meteorology*, vol. 30, no. 6, pp. 1435–1443, 2011, in Chinese.

[10] K. Kato, J. Matsumoto, and H. Iwasaki, "Diurnal variation of Cb-clusters over China and its relation to large-scale conditions in the summer of 1979," *Journal of the Meteorological Society of Japan*, vol. 73, no. 6, pp. 1219–1234, 1995.

[11] L. Yaodong, W. Yun, S. Yang, H. Liang, G. Shouting, and R. Fu, "Characteristics of summer convective systems initiated over the Tibetan Plateau. Part I: origin, track, development, and precipitation," *Journal of Applied Meteorology and Climatology*, vol. 47, no. 10, pp. 2769–2965, 2008.

[12] H. C. Lu, W. Cheng, M. Zhu, X. L. Song, and J. W. Kang, "Mechanism study of meso-scale vortex system of heavy rain in Meiyu Front," *Journal of PLA University of Science and Technology*, vol. 3, no. 4, pp. 70–76, 2002, in Chinese.

[13] Y. Q. Ni and X. J. Zhou, "Study for formation mechanism of heavy rainfall within the meiyu front along the middle and downstream of Yangtze river and theories and methods of their detection and prediction," *Acta Meteorologica Sinica*, vol. 62, no. 5, pp. 647–662, 2004, in Chinese.

[14] W. W. Song and G. P. Li, "Numerical simulation and structure characteristic analysis of a plateau vortex process," *Plateau Meteorology*, vol. 30, no. 2, pp. 267–276, 2011, in Chinese.

[15] J. H. Sun and S. X. Zhao, "A study of special circulation during Meiyu Season of the Yangtze River Basin in 1998," *Climatic and Environmental Research*, vol. 8, no. 3, pp. 291–306, 2003, in Chinese.

[16] J. Wang, Y. Yang, X. Xu, and G. Zhang, "A monitoring study of the 1998 rainstorm along the Yangtze River of China by using TIPEX data," *Advances in Atmospheric Sciences*, vol. 20, no. 3, pp. 425–436, 2003.

[17] X. D. Xu, S. Y. Tao, J. Z. Wang, L. S. Chen, L. Zhou, and X. R. Wang, "The relationship between water vapor transport features of Tibetan Plateau-monsoon "large triangle" affecting region and drought-flood abnormality of China," *Acta Meteorologica Sinica*, vol. 60, no. 3, pp. 258–264, 2002, in Chinese.

[18] S. H. Yu and W. L. Gao, "Observational analysis on the movement of vortices before/after moving out the Tibetan Plateau," *Acta Meteorologica Sinica*, vol. 64, no. 3, pp. 392–399, 2006, in Chinese.

[19] S. H. Yu, W. L. Gao, and Q. Y. Gu, "The middle-upper circulation analyses of the plateau vortex moving out of plateau and influencing flood in east China in recent years," *Plateau Meteorology*, vol. 26, no. 3, pp. 466–475, 2007, in Chinese.

[20] S. X. Zhao and S. M. Fu, "An analysis on the southwest vortex and its environment fields during heavy rainfall in eastern Sichuan Province and Chongqing in September 2004," *Chinese Journal of Atmospheric Sciences*, vol. 31, no. 6, pp. 1059–1075, 2007, in Chinese.

[21] Y. Zhao and Y. F. Qian, "Relationship between the Tibetan Plateau surface thermal anomalies and the summer circulation over East Asia and rainfall in the Yangtze and Huaihe River areas," *Acta Meteorologica Sinica*, vol. 67, no. 3, pp. 397–406, 2009, in Chinese.

[22] X. D. Xu and L. S. Chen, "Progress in experimental research on Qinghai Tibet Plateau atmospheric science," *Journal of Applied Meteorological Science*, vol. 17, no. 6, pp. 756–772, 2006, in Chinese.

[23] S. Y. Tao and Y. H. Ding, "Observational evidence of the influence of the Qinghai-Xizang (Tibet) Plateau on the occurrence of heavy rain and severe convective storms in China," *Bulletin of the American Meteorological Society*, vol. 62, no. 1, pp. 23–30, 1981.

[24] Z. Wang, A. Duan, and G. Wu, "Time-lagged impact of spring sensible heat over the Tibetan Plateau on the summer rainfall anomaly in East China: case studies using the WRF model," *Climate Dynamics*, vol. 42, no. 11-12, pp. 2885–2898, 2013.

[25] H. X. Duan, W. S. Lu, and B. G. Bi, "Impact of the condensation heating and surface heat flux on a rainstorm event of southwest vortex," *Plateau Meteorology*, vol. 27, no. 6, pp. 1315–1321, 2008, in Chinese.

[26] Y. H. Kuo, L. Cheng, and R. A. Anthes, "Mesoscale analyses of Sichuan flood catastrophe 11–15 July 1981," *Monthly Weather Review*, vol. 114, no. 11, pp. 1984–2003, 1986.

[27] Y. H. Kuo, L. Cheng, and J. W. Bao, "Numerical simulation of the 1981 Sichuan flood. Part I: evolution of a mesoscale southwest vortex," *Monthly Weather Review*, vol. 116, no. 12, pp. 2481–2504, 1988.

[28] T. Chen, F. H. Zhang, and Y. H. Duan, "A study of relationship between a southwest vortex and the mesoscale convective systems during the severe "6.12" rainstorm event in Guangxi province," *Acta Meteorologica Sinica*, vol. 69, no. 3, pp. 472–485, 2009, in Chinese.

[29] Y. C. Zhao and Y. H. Wang, "A case study on plateau vortex inducing southwest vortex and producing extremely heavy rain," *Plateau Meteorology*, vol. 29, no. 4, pp. 819–831, 2010, in Chinese.

[30] E. J. Mlawer, S. J. Taubman, P. D. Brown, M. J. Iacono, and S. A. Clough, "Radiative transfer for inhomogeneous atmospheres: RRTM, a validated correlated-k model for the longwave," *Journal of Geophysical Research: Atmospheres*, vol. 102, pp. 16663–16682, 1997.

[31] J. Dudhia, "Numerical study of convection observed during the winter monsoon experiment using a mesoscale two-dimensional model," *Journal of the Atmospheric Sciences*, vol. 46, pp. 3077–3107, 1989.

[32] A. C. M. Beljaars, "The parameterization of surface fluxes in large-scale models under free convection," *Quarterly Journal of the Royal Meteorological Society*, vol. 121, no. 522, pp. 255–270, 1994.

[33] M. Tewari, F. Chen, W. Wang et al., "Implementation and verification of the unified NOAH land surface model in the WRF model," in *Proceedings of the 20th Conference on Weather Analysis and Forecasting/16th Conference on Numerical Weather Prediction*, pp. 11–15, Seattle, WA, USA, January 2004.

[34] S.-Y. Hong, Y. Noh, and J. Dudhia, "A new vertical diffusion package with an explicit treatment of entrainment processes," *Monthly Weather Review*, vol. 134, no. 9, pp. 2318–2341, 2006.

[35] G. A. Grell and D. Devenyi, "A generalized approach to parameterizing convection combining ensemble and data assimilation techniques," *Geophysical Research Letters*, vol. 29, no. 14, 2002.

[36] J. A. Milbrandt and M. K. Yau, "A multimoment bulk microphysics parameterization. Part I: analysis of the role of the spectral shape parameter," *Journal of the Atmospheric Sciences*, vol. 62, no. 9, pp. 3051–3064, 2005.

[37] J. A. Milbrandt and M. K. Yau, "A multimoment bulk microphysics parameterization. Part II: a proposed three-moment closure and scheme description," *Journal of the Atmospheric Sciences*, vol. 62, no. 9, pp. 3065–3081, 2005.

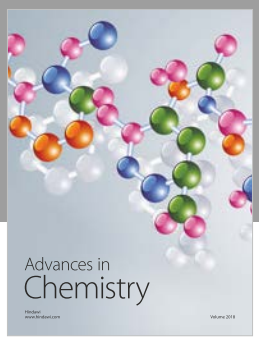

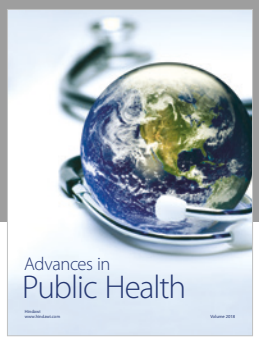

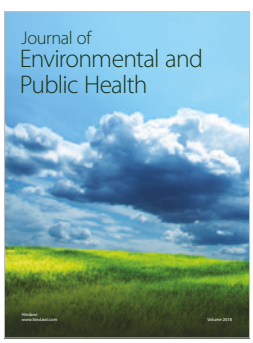

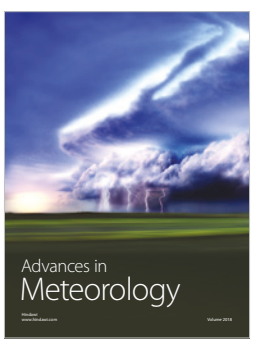

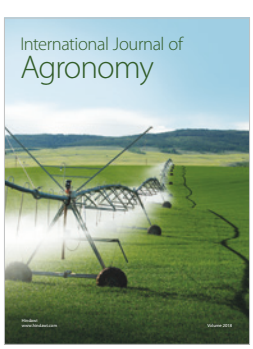

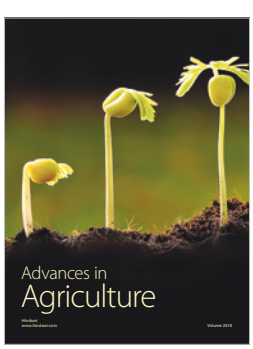

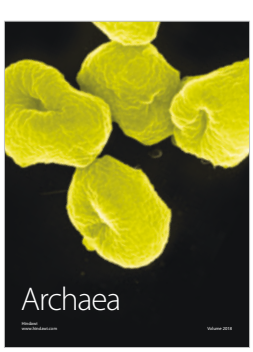

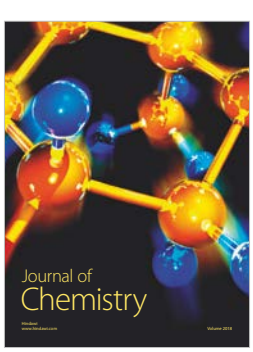


Hindawi

Submit your manuscripts at
www.hindawi.com